Mechanics of Materials 122 (2018) 96–103

Contents lists available at ScienceDirect

Mechanics of Materials

journal homepage: www.elsevier.com/locate/mechmat

Research paper

Simulation of anisotropic load transfer and stress distribution in sicp/Al composites subjected to tensile loading

Zhang J.F.[a,b], Zhang X.X.[a,*], Wang Q.Z.[a], Xiao B.L.[a,*], Ma Z.Y.[a]

[a] Shenyang National Laboratory for Materials Science, Institute of Metal Research, Chinese Academy of Sciences, 72 Wenhua Road, Shenyang 110016, China
[b] University of Chinese Academy of Sciences, 19 Yuquan Road, Beijing 100049, China

ARTICLE INFO

Keywords:
Metal matrix composites (MMCs)
Load transfer
Finite element (FE) analysis
Load-rebalancing
Representative volume element (RVE)
Stress concentration factor

ABSTRACT

The deformation behaviors of 17 vol% SiCp/2009Al composite plates were studied by using microscale finite element (FE) models. The effects of aspect ratio (AR) of SiC particles were investigated. Tensile results obtained from experiments and simulations matched well. The load transfer and stress distribution between SiC particles and metal matrix were studied by calculating the mean stress in each phase. We found that, in the longitudinal direction, increasing the AR of SiC particles increased the mean stress in the SiC particles and decreased that in the metal matrix. Evolution of the stress concentration factor for each phase was obtained from simulation and a load-rebalancing phenomenon was observed. Stress concentration factor of SiC went down around the middle of the elastic stage (true strain value equals to 0.0025) and reversed at the beginning of the plastic stage of tension.

1. Introduction

Metal matrix composites (MMCs) exhibit distinct advantages over unreinforced metals and alloys, such as high stiffness and strength, distinguished wear resistance, attractive fatigue properties, and superior thermal and electrical characteristics (Heidary and Akhlaghi, 2011; Zhang et al., 2015; Zhou et al., 2016).

Due to the high performance of MMCs, design of MMCs has captured the attention of the MMC community. To guarantee high accuracy of material design, a good understanding of micro mechanics of MMCs is critical. The micro mechanics of MMCs has been explored over the past decades (Dong et al., 2015; Ju and Sun, 2001; Laschet et al., 2017). Among the MMCs, particles reinforced MMCs (PRMMCs) are widely used due to their good formability and machinability. After experiencing platic working, such as extrusion, rolling or forging (Luk et al., 2015; Zhang et al., 2016a,b), anisotropy generally appeared in the PRMMCs due to the preferred alignment of particles. For example, the extruded SiCp/2020Al composite exhibited higher Young's modulus and tensile strength along the extrusion direction than perpendicular to the transverse direction (Ganesh and Chawla, 2005). This may cause inhomogeneous deformation, or lead to unexpected failure, when an external load is applied (Banabic, 2016). Hence, to optimize the manufacturing processes and guaranty the final properties, it is important to study the anisotropy effects and the inner stress/strain transformation of PRMMCs quantitatively during plastic deformation.

By applying the neutron and synchrotron X-ray diffraction methods (Daymond et al., 2005; Garces et al., 2007; Wilkes et al., 2009; Young et al., 2009; Zhang et al., 2016c), the internal strains and stresses in PRMMCs can be determined. Garces et al. (2007) measured the evolution of stress via neutron diffraction in the matrix of short fibers reinforced MMCs during in situ uniaxial deformation. Roy et al. (2011) measured the lattice strains in all three phases of the Al_2O_3 reinforced AlSi12 composite during tension and compression deformation via energy dispersive synchrotron X-ray diffraction. They found that the stress concentration factor of the reinforcement decreased during elastic deformation stage and followed by a continuous increase during plastic deformation stage. The stress concentration factor of the matrix varied inversely. Although these methods can provide experimental data of strains and stresses, it is still difficult and expensive to conduct neutron or synchrotron X-ray diffraction.

In addition to experimental investigations, computer simulation is another useful method of studying the load transfer and quantifying local stresses and strains in PRMMCs, especially at the microscale (Meyer and Waas, 2016; Sharma et al., 2016; Zhang et al., 2016b). Therefore, utilizing computer simulation approach to quantify the internal stress and stress concentration factor of PRMMCs can reduce the cost of investigation. Zhang et al. (2017) used finite element method to study the interface strength of SiCp reinforced aluminum matrix composite. They studied the inner stress in each phase of the composite. However, the anisotropy effects of the composite were not addressed. Chawla et al. (2006) reconstructed a 3D microstructure model of a SiCp/2080Al composite via serial sectioning method, based on which a

* Corresponding authors.
E-mail addresses: xxzhang@imr.ac.cn (X.X. Zhang), blxiao@imr.ac.cn (B.L. Xiao).

https://doi.org/10.1016/j.mechmat.2018.04.011
Received 24 October 2017; Received in revised form 29 March 2018; Accepted 12 April 2018
Available online 13 April 2018

Nomenclature

σ	The flow stress
f	A non-dimensional function determined from the uniaxial tensile test
σ_{ref}	A reference stress
$\Delta\sigma_y$	The increment of yield strength of the matrix caused by the quenching hardening effect (Qu et al., 2005; Shao et al., 2011)
σ_y	The initial yield strength
K, n	The parameters describing work-hardening
ε^p	The equivalent plastic strain
β	A constant equal to 2.7 (Nan and Clarke, 1996)
μ	The shear modulus
b	The Burgers vector of the matrix
ΔCTE	The difference between the coefficients of thermal expansion of the matrix and the particles
ΔT	The temperature difference because of quenching
V_f	The volume fraction of the particles
d	The diameter of the particles

finite element model was developed to investigate the anisotropic character of the composite. However, such an approach can only develop a micromechanical model based on real composites, but not virtual composites. Therefore, it is difficult to construct models with different degrees of anisotropy. Besides, it requires many labor works and is very time-consuming. Due to those limitations, the anisotropy effects on the internal stress and stress concentration factors of the PRMMCs were not well studied.

In this study, simulation method was applied to study the micro mechanics in a SiCp/Al composite. A series of 3D models of virtual SiCp/Al composites generated via computer simulation method were employed to study the load transfer, internal strain and stress in the composites. Three different aspect ratios (1, 2.5 and 4) of particles were investigated to characterize the effect of the morphology of SiC particles, which introduce anisotropy effects into the virtual composites. The internal stresses in the metal matrix and the reinforcement were computed to study the load transfer and stress distribution of the composites.

2. Experimental and computational approaches

2.1. Material preparation and mechanical property test

In this work, 17 vol.% SiCp/2009Al composite plates were used. The nominal average diameter of SiC particles was 7 μm. The composites were manufactured using vacuum hot pressing at 580 °C and then hot rolled from 20 into 3 mm thick plates at 480 °C. This rolling process introduces anisotropy into the composites. The rolled composite plates were solution treated 2 h at 500 °C. Subsequently, it was treated by water quenching and natural aging for four days. A 2009Al plate was also fabricated following the same route for the purpose of comparison.

Two sets of tensile specimens with a thickness of 3 mm and gauge length of 20 mm were machined from these rolled composite plates. The tension direction of one set was along the longitudinal direction (rolling direction), while that of another set was along the transverse direction. The uniaxial tensile tests were performed at room temperature and the strain rate was set as $1.6 \times 10^{-3}\ s^{-1}$. Two sets of 2009Al plates were also tested via uniaxial tension.

2.2. Microstructures of SiC particles in sicp/2009Al plate

A series of 3D microstructure-based representative volume elements (RVEs) were studied in this work. Due to the anisotropy of rolling sheets, as shown in Fig. 1, the alignments and aspect ratios of SiC particles should be characterized. Statistical information about the diameters, aspect ratios, and the angles between longitudinal direction and long axes of particles were established based on the metallographs, as shown in Fig. 1(d). Fig. 1(a) showed a preferred orientation of SiC particles parallel to the longitudinal direction. The 3D microstructure-based RVEs of the composites were created based on these data. These

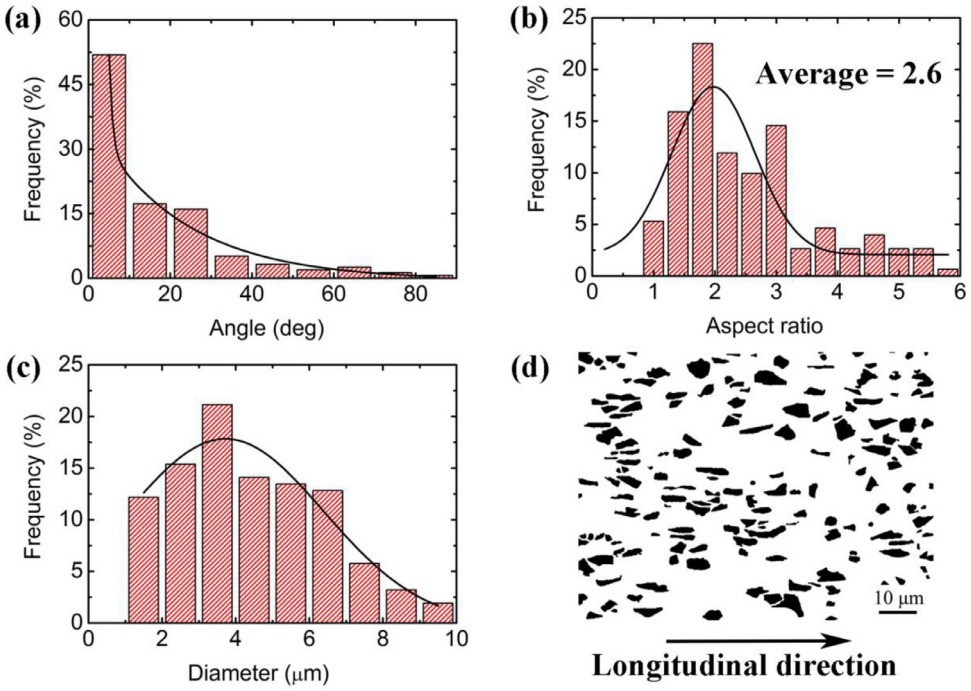

Fig. 1. The statistical result of the particles in SiCp/2009Al rolling sheets along longitudinal direction. (a) The statistic data of angle between longitudinal direction and long axes of SiC particles, (b) aspect ratio and (c) the diameter of SiC particles and the (d) metallograph of 17 vol.% SiCp/2009 Al composite rolling plates.

virtual models were created using the integrated random cutting and random sequential adsorption approach proposed in the Ref. Zhang et al. (2014b). The volume frictions of SiC particles in these models were set to 17 vol.%.

The size factor of these RVE models was defined as:

$$\delta = 2L/D \tag{1}$$

where L the side length of the microstructure domain and D is the mean diameter of the particles. In this work, the size factors of all models were selected as 5 (Zhang et al., 2014a). As Harper et al. (2012), Kanit et al. (2003) revealed, models based on RVEs with large sizes generally produced smaller errors and converged to the true target properties. However, models based on RVEs with large sizes require many computational resources and are time-consuming. As Kanit et al. (2003) has shown, models based on RVEs with medium size can also produce results with acceptable errors by using several different RVEs with the same size. In the present study, we chose the models whose computer memory requirement is less than 16 GB due to the limitation of the computer hardware, and models based on RVEs with size factor of five require the computer memory of about 15 GB. Therefore, the size factor of five was used in this study. To improve the computational accuracy, models for each aspect ratio are repeated three times using three different RVEs with same size factor.

SiC particles in RVEs were randomly cut from cuboid primitive objects (Zhang et al., 2014b). To characterize different aspect ratios of SiC particles in SiCp/2009Al composite plates, three different aspect ratios of the primitive object of SiC particles were chosen. They were 1, 2.5 and 4, respectively. According to Fig. 1(a), the long axes of all SiC particles aligned along the rolling direction, i.e. the Y direction, as shown in Fig. 2. According to Fig. 1(b), the aspect ratio of 2.5 is close to the aspect ratio of the particles obtained from metallograph. According to the nominal average diameter of the raw SiC particles in this composite, the average diameter of SiC particles was set to 7 μm according to the Ref. Zhang et al. (2014b).

The mesh type of all RVEs was unstructured 4-nodes tetrahedrons, and TetGen (Si, 2015) was used to generate those meshes. We used the maximum tetrahedron volume constraint to control the mesh size and the mesh size effects will be assessed in Section 3.1.

2.3. Constitutive behaviors

In this work, the metal matrix of SiCp/2009Al composite was defined as an elastoplastic material. The SiC particles were defined as an ideal elastic material. The relation between the flow stress and the plastic strain of the 2009Al matrix was expressed as (Arsenault et al., 1991; Chakrabarty and Drugan, 1988; Nan and Clarke, 1996):

$$\sigma = \sigma_{ref} f(\varepsilon^p) + \Delta\sigma_y = \sigma_y + K(\varepsilon^p)^n + \Delta\sigma_y \tag{2}$$

$$\Delta\sigma_y = \beta\mu\sqrt{6|\Delta CTE||\Delta T|\frac{V_f}{1-V_f}\frac{b}{d}} \tag{3}$$

Definitions of all symbols are listed and explained in Nomenclature.

Some material parameters of 2009Al were obtained from uniaxial tensile tests, σ_y = 308 MPa, K = 408 MPa, and n = 0.45. Other parameters of 2009Al were obtained from the literature (Kipp, 2010): Young's modulus and Poisson's ratio were set to be 75 GPa and 0.33, respectively. The Young's modulus and Poisson's ratio of SiC particles were set to be 427 GPa and 0.17, respectively (Munro, 1997).

2.4. Loads and boundary conditions

Two different loading conditions were adopted according to the alignments of SiC particles. As illustrated in Fig. 3, these models were subjected to uniaxial tension by defining a fixed surface on one side and a loading surface on the opposite side. In addition, the uniaxial tension of one set was along the longitudinal direction (Y axis in Fig. 3) while that of another set was along the transverse direction (Z axis in Fig. 3). Except the loading surface and the fixed surface, other surfaces are set to free boundary conditions.

To characterize the load transfer, by using the rule of mixture, the effective stress of composite can be expressed as:

$$\sigma_{eff} = (V_{SiC}\sigma_{SiC} + V_{Matrix}\sigma_{Matrix})/V_{Composite} \tag{4}$$

where σ_{eff} is the effective stress of the 3D RVE based finite element models (RVE-FEm), V_{SiC} and V_{Matrix} the volume of the SiC particles and the metal matrix, respectively, σ_{SiC} and σ_{Matrix} the average stress of the SiC particles and the metal matrix, respectively, and $V_{Composite}$ the total volume of the composite.

By extending the rule of mixture, the average stress of SiC particles can be expressed as:

$$\sigma_{SiC} = \frac{\sum_1^n V_i\sigma_i}{\sum_1^n V_i} \tag{5}$$

where n is the number of elements in all SiC particles, V_i and σ_i the volume and stress of each element in all SiC particles, respectively. Similarly, the average stress of metal matrix σ_{Matrix} can be defined.

To describe the inhomogeneity of stress between the phases in PRMMCs, a stress concentration factor (Roy et al., 2011; Zhang et al., 2017) of SiC particles was introduced and defined as

$$R_{SiC} = \frac{\sigma_{SiC}}{\sigma_{eff}} \tag{6}$$

where σ_{SiC} is the average stress of SiC particles, and σ_{eff} the effective stress of the RVE-FEm. Similarly, the stress concentration factor of metal matrix R_{Matrix} can be obtained.

3. Computational results and discussion

3.1. Mesh size effects

In this work, four different mesh sizes were investigated to assess

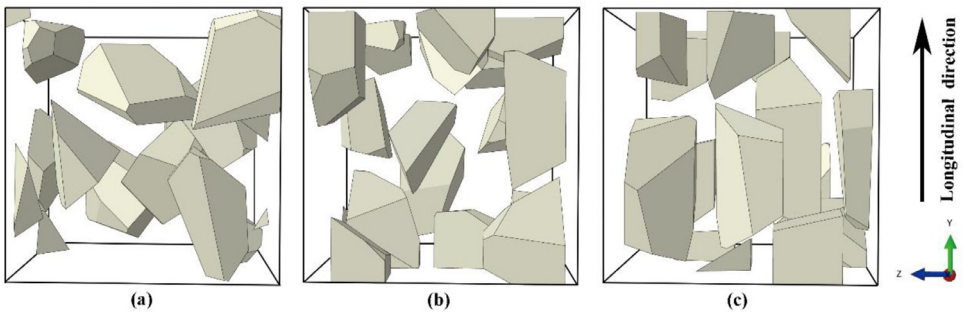

Fig. 2. The microstructure-based representative volume element models of the 17 vol.% SiCp/2009Al. The aspect ratios of SiC particles primitive objects of (a) was 1, (b) 2.5 and (c) 4.

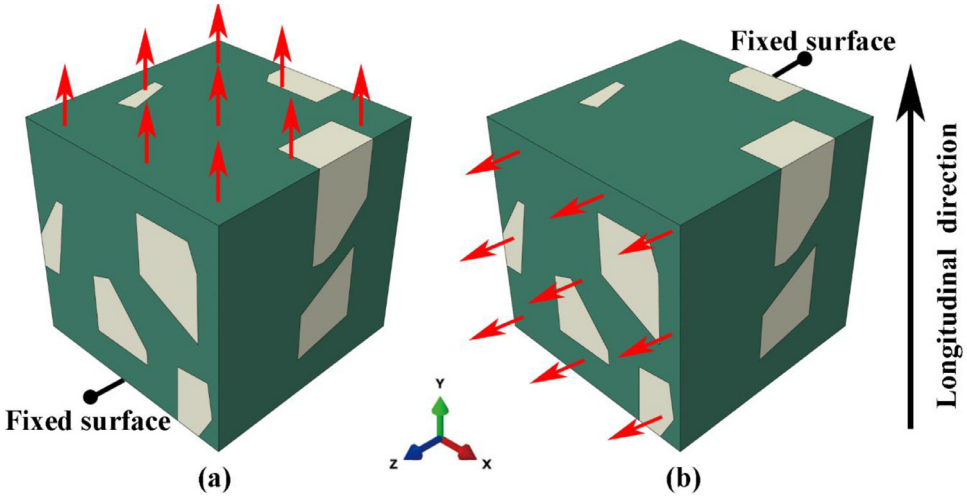

Fig. 3. Tow different loading conditions of the RVE models. (a) Tension was along the longitudinal direction and (b) tension was along the transverse direction.

the mesh size effect. The mesh size was controlled by the maximum tetrahedron volume constraint (a) in TetGen (Si, 2015). a was 0.05, 0.01, 0.005 and 0.0025 in the four models, respectively.

As shown in Fig. 4(a), the model with finer mesh predicted lower flow stress. From Figs. 4(a)–(d), it can be found that the finer mesh model could describe more details of deformation of metal matrix, especially around SiC particles. When a was less than 0.01, the predicted strain-stress curves tend to be stable. At the true strain 0.06, the stress values of model with the mesh size 0.05, 0.01, 0.005 and 0.0025 are 604, 569, 564 and 553 MPa, respectively. If we take the stress value of model with the mesh size 0.0025 as the level of 100%, then the stress values of model with the mesh size of 0.05, 0.01 and 0.005 have the levels of 109.2%, 102.9% and 101.9%, respectively. Although finer mesh size increases the computational accuracy, it leads to higher computational cost. On the balance of computational accuracy and cost, the maximum tetrahedron volume of 0.005 was chosen in this work.

3.2. Tensile strength of RVE-FEm

As mentioned in Sections 2.2 and 2.4, two sets of models with two different loading directions (longitudinal and transverse directions) were employed in this work. Moreover, three different aspect ratios (AR1, AR2.5 and AR4) of SiC particles were studied in each set of models. To obtain accurate predictions (Kanit et al., 2003), three models with the same loading direction and aspect ratio were simulated in this study. Fig. 5 presented the simulation results of uniaxial tensile tests of these models. In Fig. 5(a), when the tensile direction was along the longitudinal direction, flow stress increased with increasing the aspect ratios of SiC particles. In Fig. 5(b), when the tensile direction was along the transverse direction, similar relation between aspect ratios and flow stresses could be also observed but not as obviously as that along the longitudinal direction.

To investigate the anisotropy of the different models, flow stress curves of models with different loading directions were computed and

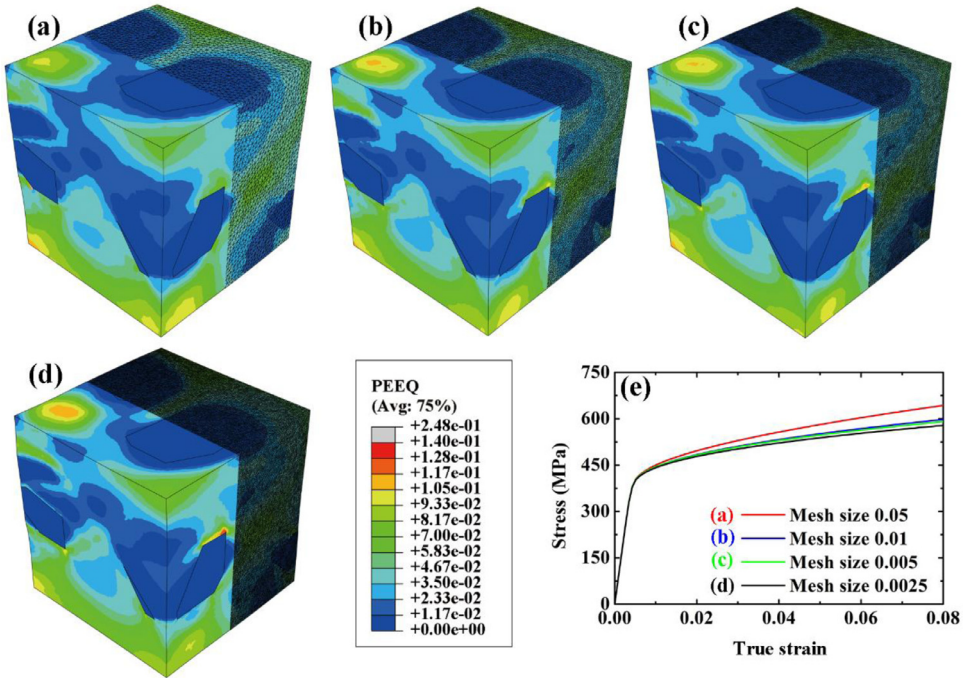

Fig. 4. The equivalent plastic strain of models at the total strain equals to 0.04 with mesh size of (a) 0.05, (b) 0.01, (c) 0.005 and (d) 0.0025. The back halves of these four pictures showed their meshes. (e) The strain-stress curves obtained from models with four different mesh size.

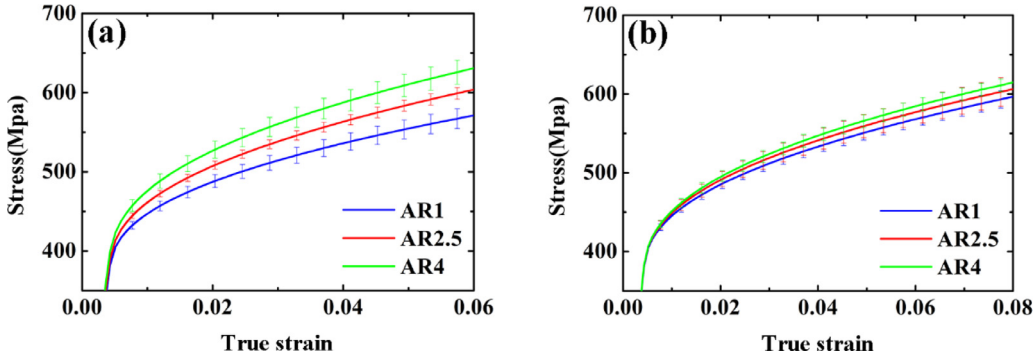

Fig. 5. The strain-stress curves from simulation of uniaxial tension of SiCp/2009Al composite rolling plates. (a) Tensile directions were along the longitudinal direction and (b) along the transverse direction.

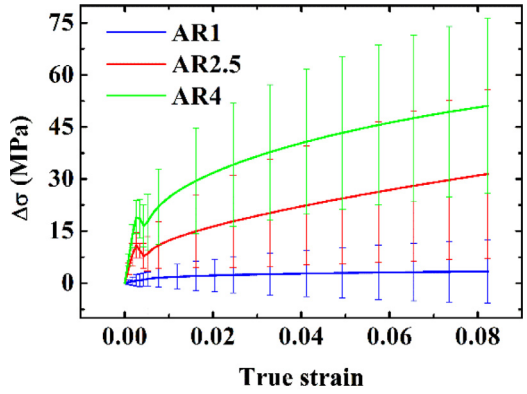

Fig. 6. In models with 3 different aspect ratios of SiC particles, the difference values between flow stresses obtained from tension along the longitudinal direction and along the transverse direction.

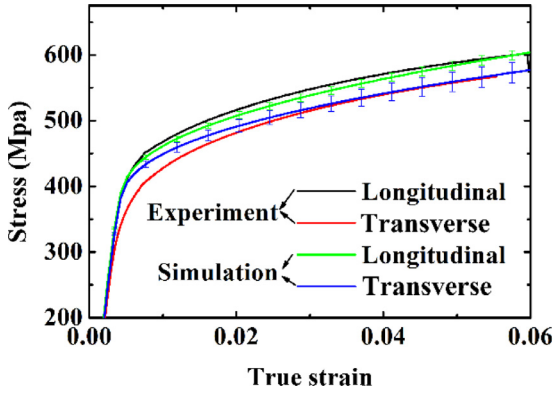

Fig. 7. The comparison between experimental and simulative tensile tests results. The experiment results were obtained from tensile test of 17 vol.% SiCp/2014Al. The simulation results were obtained from models with aspect ratio 2.5 (AR2.5).

are shown in Fig. 6. As the aspect ratio of SiC particles increased, the different values between flow stresses along the longitudinal and transverse direction increased.

According to Fig. 1(b), we chose the models with AR2.5 of SiC particles to predict the tensile tests results of 17 vol.% SiCp/2009Al composite plates. Fig. 7 shows the results of simulations and experiments. The simulation results matched well with the experiment results. According to Fig. 7, the tensile test went into plastic stage earlier for the tension along the longitudinal direction compared to that along the transverse direction. It resulted in the fluctuations of the curves of AR2.5 and AR4 at the true strain around 0.005, as shown in Fig. 6.

3.3. Stress evolution in SiC particles and metal matrix

Based on Eq. (5), the stress evolutions of the SiC and metal matrix along the loading direction were obtained and are shown in Fig. 8. Fig. 8(a) and (b) shows that for tensions along the longitudinal direction, the stress increased in the SiC particles and decreased in the matrix with the raising the aspect ratios of SiC particles. In other words, with higher aspect ratio of SiC particles, they carried more loads while the matrix carried less load, agreeing with previous studies (Ganesh and Chawla, 2005; Luk et al., 2015; Zhang et al., 2016a,b). Fig. 8(c) and (d) shows that for the tensions along the transverse direction, the stresses in SiC particles with different aspect ratios almost had similar values. However, in contrast to the tensions along the longitudinal direction, the stress in the matrix along the transverse direction increased with raising the aspect ratio of SiC particles. It reveals that with higher aspect ratios of SiC particles, the matrix carried more load when the load direction was along the transverse direction.

3.4. Stress concentration factors of SiC particles and metal matrix

Based on Eq. (6), the stress concentration factors of the SiC and metal matrix along the loading direction were obtained and are shown in Fig. 9. It shows that in the tensions along the longitudinal direction, the stress concentration factors of SiC increased and that of the matrix decreased with raising the aspect ratios of SiC particles. However, this relationship reversed in the tensions along the transverse direction as shown in Fig. 9(c) and (d). Similar to Fig. 8(c) and (d), the differences between stress concentration factors were small in the tensions along the transverse direction.

Fig. 9 shows that R_{SiC} is always much higher than R_{Matrix}. According to the reference Shi et al. (2016), this is due to that the Young's modulus of SiC is much larger than that of metal matrix. R_{SiC} decreased and R_{Matrix} increased during elastic deformation. R_{SiC} increased and R_{Matrix} decreased during plastic deformation. This reveals that the load carried by SiC particles decreased during elastic deformation and increased during plastic deformation. The variation of the load carried by the matrix was opposite. We may call this effect that the stress concentration factor changed during deformations as load-rebalancing.

3.5. Load-rebalancing in composites

The evolutions of phase stress concentration factors were coincident with the measurements via energy dispersive synchrotron X-ray diffraction by Roy et al. (2011), as shown in Fig. 10. To show the details of load-rebalancing in the composites, Fig. 11(a) and (b) gives the detailed views of Fig. 9(a) and (c). It is obvious that the load-rebalancing began at the middle of the elastic stage, and reversed at the beginning of the plastic stage. In this work, the load-rebalancing began at a true strain around 0.0025 and reversed at a true strain around 0.005.

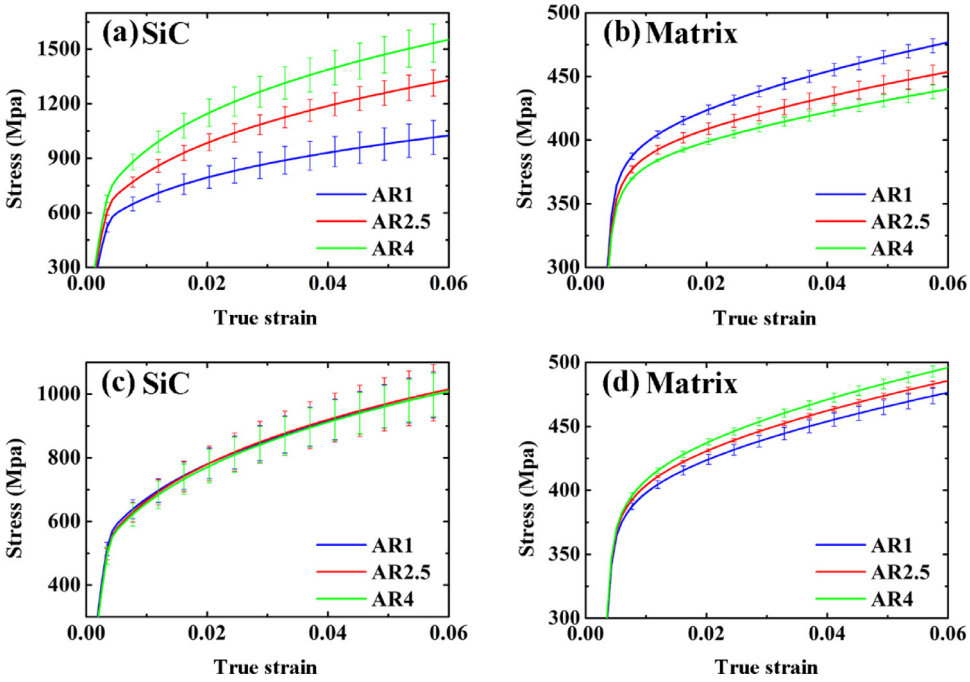

Fig. 8. (a) and (b) are the volumetric average stress evolution in SiC and matrix with the tension along the longitudinal direction, (c) and (d) the volumetric average stress evolution in SiC and matrix with the tension along the transverse direction.

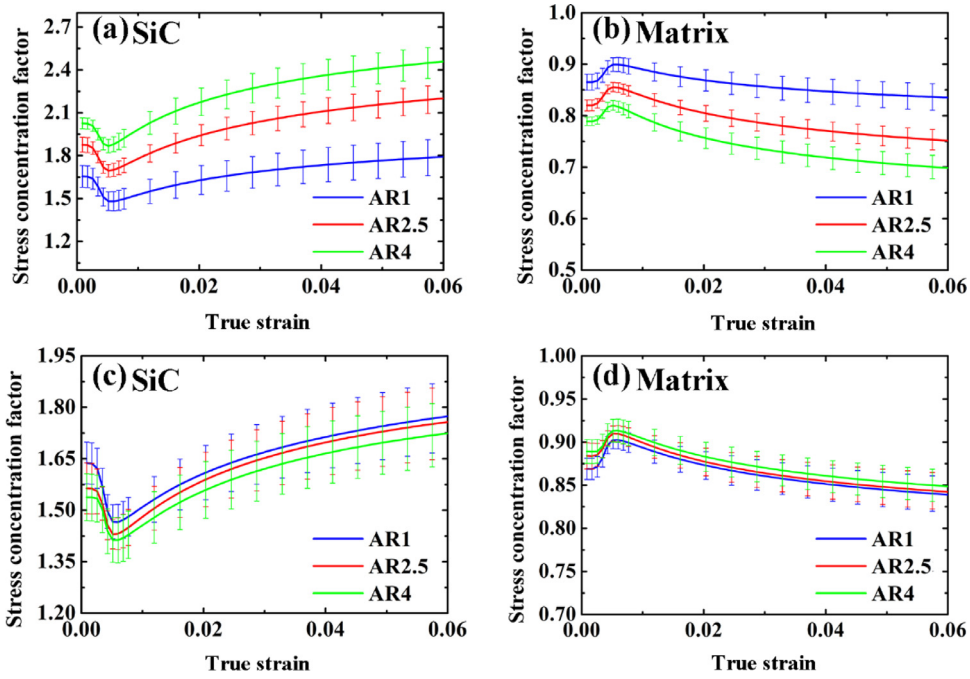

Fig. 9. (a) and (b) are the stress concentration factor evolution in SiC and matrix with the tension along the longitudinal direction, (c) and (d) the stress concentration factor evolution in SiC and matrix with the tension along the transverse direction.

From Eq. (4), we can obtain:

$$\sigma_{eff} = f_{SiC}\sigma_{SiC} + f_{Matrix}\sigma_{Matrix} \tag{7}$$

where f_{SiC} and f_{Matrix} are the volume fractions of the SiC particles (17%) and the metal matrix (83%), respectively. Combing Eq. (7) with Eq. (6):

$$1 = f_{SiC}R_{SiC} + f_{Matrix}R_{Matrix} \tag{8}$$

Because f_{SiC} and f_{Matrix} in Eq. (8) were fixed in this work, the stress concentration factors of SiC particles and metal matrix were negatively correlated.

Fig. 11(c) and (d) shows that the elastic zone volume fraction decreased sharply at the beginning points and gently at the reversing points of load-rebalancing, no matter the tension direction was along the longitudinal direction or the transverse direction. The reason why the rebalancing happened in the middle of the elastic of deformation was related to the elastoplastic deformation of metal matrix during the tension of composites.

Fig. 12 shows the elastic zone distribution in the metal matrix at the beginning and reversing points of the load-rebalancing. It reveals that in the second half of elastic deformation stage of the composite, more

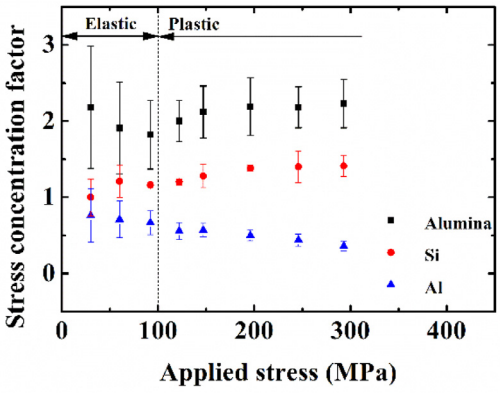

Fig. 10. Stress concentration factors of Al_2O_3 reinforced AlSi12 composite in individual phases as a function of applied tensile stress (Roy et al., 2011).

deformation took place in the metal matrix. Therefore, at the beginning of the load-rebalancing, R_{Matrix} went up and R_{SiC} went down. At the reversing points of load-rebalancing, most area of metal matrix was in the plastic stage. Accordingly, the stress level of metal matrix would not go sharply up because of the plastic flow of metal matrix. Then, R_{Matrix} went down and R_{SiC} went up at the reversing points.

In summary, the plasticity of metal matrix was the primary cause of the load-rebalancing in composites.

3.6. Limitations of the present FE models

This FE model shows great feasibility in simulating the load transfer and stress distribution of SiCp/2009Al composite. The aspect ratios and directions of SiC particles were taken into consideration, and their effects on the load transfer and stress distribution were discussed. However, there are still some inaccuracies of these models. For instance, the yield stress from the simulation is higher than that of the experiment for the transverse direction in Fig. 7. This is cause by some limitations of these models. The major limitations are:

(1) To simplify the problems of this work, the effects of interface were not taken into consideration. Many investigations have already shown that the mechanical properties of the interface affected the simulation results of MMCs (Ferguson et al., 2014; Shao et al.,

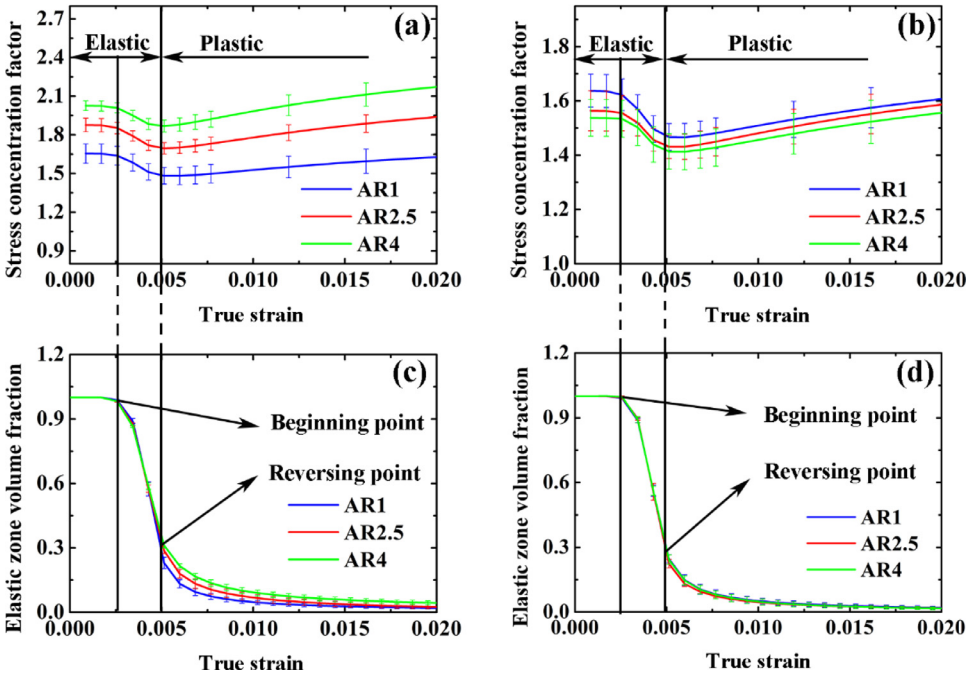

Fig. 11. The relationships between stress concentration factors and elastic zone volume fractions of metal matrix. (a) and (c) were the stress concentration factor and elastic zone volume fraction evolution when the tension was along the longitudinal direction. (b) and (d) were the stress concentration factor and elastic zone volume fraction evolution when the tension was along the transverse direction.

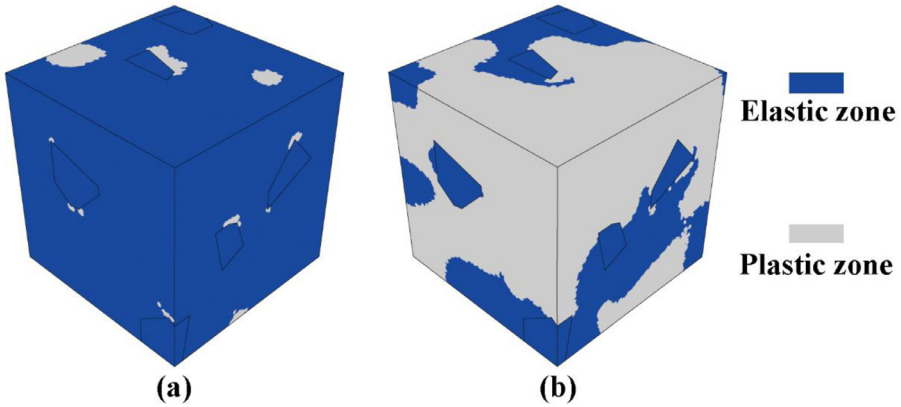

Fig. 12. The elastic and plastic zone in metal matrix distribution at (a) the beginning points of and (b) the reversing points of load rebalancing. And this model had SiC particles of aspect ratio of 2.5 and subjected to tension along longitudinal direction.

2011; Zhang et al., 2016a).

(2) The geometrical mismatch (Huang et al., 2004) of metal matrix during deformation was not considered in this work. The thermal mismatch generated during quenching was assumed to affect the entire matrix zone. However, when the particle volume fraction is lower than 25%, not all the part of the matrix was affected by thermal mismatch (Shao et al., 2011; Shibata et al., 1992; Taya et al., 1991). These two factors would introduce errors in constitutive behaviors of metal matrix.

4. Conclusions

In this work, a series of RVE-FEm with considering the aspect ratio and direction of SiC particles were developed to predict the elasto-plasticity and anisotropy of 17 vol.% SiCp/2009Al composite plates. The effects of aspect ratio of SiC particles were investigated. The mechanical properties along different directions of the composite plates were simulated. A load-rebalancing phenomenon was observed that the stress concentration factor of the matrix increased during the elastic deformation stage and decreased during the plastic deformation stage. Based on the computational simulation results, following conclusions can be made:

(1) When the tension was along the longitudinal direction, the stress concentration factor of reinforcements increased with increasing the aspect ratio of SiC particles. However, the aspect ratios and directions of SiC particles affected the stress concentration factor slightly when the tension was along the transverse direction.
(2) With the long axis of SiC particles aligning along the longitudinal direction, the SiC particles with higher aspect ratios carry more load in the longitudinal direction, but less load in the transverse direction.
(3) The load-rebalancing phenomenon was caused by the plastic deformation of the metal matrix. When most of the metal matrix started to go into plastic deformation, the load-rebalancing began. When most of metal matrix had already went into plastic deformation, the load-rebalancing reversed.

Acknowledgments

The authors gratefully acknowledge support from the National Key R&D Program of China under grant No. 2017YFB0703104 and the National Natural Science Foundation of China under grant No. 51671191 and No. 51401219.

Supplementary materials

Supplementary material associated with this article can be found, in the online version, at doi:10.1016/j.mechmat.2018.04.011.

References

Arsenault, R.J., Wang, L., Feng, C.R., 1991. Strengthening of composites due to microstructural changes in the matrix. Acta Metall. Mater. 39, 47–57.
Banabic, D., 2016. Advances in plastic anisotropy and forming limits in sheet metal forming. J. Manuf. Sci. Eng. 138, 090801.
Chakrabarty, J.S., Drugan, W.J., 1988. Theory of plasticity. J. Appl. Mech 55 253–253.
Chawla, N., Sidhu, R.S., Ganesh, V.V., 2006. Three-dimensional visualization and micro structure-based modeling of deformation in particle-reinforced composites. Acta Mater 54, 1541–1548.
Daymond, M.R., Hartig, C., Mecking, H., 2005. Interphase and intergranular stress generation in composites exhibiting plasticity in both phases. Acta Mater 53, 2805–2813.
Dong, S., Zhou, J., Liu, H., Wu, Y., Qi, D., 2015. The strengthening effect of carbon nanotube in metal matrix composites considering interphase. Mech Mater. 91, 1–11.
Ferguson, J.B., Thao, X., Rohatgi, P.K., Cho, K., Kim, C.S., 2014. Computational and analytical prediction of the elastic modulus and yield stress in particulate-reinforced metal matrix composites. Scripta Mater. 83, 45–48.
Ganesh, V.V., Chawla, N., 2005. Effect of particle orientation anisotropy on the tensile behavior of metal matrix composites: experiments and micro structure-based simulation. Mater. Sci. Eng. A 391, 342–353.
Garces, G., Bruno, G., Wanner, A., 2007. Load transfer in short fibre reinforced metal matrix composites. Acta Mater. 55, 5389–5400.
Harper, L., Qian, C., Turner, T., Li, S., Warrior, N., 2012. Representative volume elements for discontinuous carbon fibre composites–part 2: determining the critical size. Compos. Sci. Technol. 72, 204–210.
Heidary, D.S.B., Akhlaghi, F., 2011. Theoretical and experimental study on settling of SiC particles in composite slurries of aluminum A356/SiC. Acta Mater. 59, 4556–4568.
Huang, Y., Qu, S., Hwang, K.C., Li, M., Gao, H., 2004. A conventional theory of mechanism-based strain gradient plasticity. Int. J. Plast. 20, 753–782.
Ju, J.W., Sun, L.Z., 2001. Effective elastoplastic behavior of metal matrix composites containing randomly located aligned spheroidal inhomogeneities. Part I: micro-mechanics-based formulation. Int. J. Solids Struct. 38, 183–201.
Kanit, T., Forest, S., Galliet, I., Mounoury, V., Jeulin, D., 2003. Determination of the size of the representative volume element for random composites: statistical and numerical approach. Int. J. Solids Struct. 40, 3647–3679.
Kipp, D.O., 2010. Metal Material Data Sheets. MatWeb, LLC.. http://app.knovel.com/hotlink/toc/id:kpMMDS0002/metal-material-data-sheets/metal-material-data-sheets (Accessed 12 September 2016).
Laschet, G., Spekowius, M., Spina, R., Hopmann, C., 2017. Multiscale simulation to predict microstructure dependent effective elastic properties of an injection molded polypropylene component. Mech. Mater. 105, 123–137.
Luk, M.J., Mirza, F.A., Chen, D.L., Ni, D.R., Xiao, B.L., Ma, Z.Y., 2015. Low cycle fatigue of SiCp reinforced AA2009 composites. Mater. Des. 66, 274–283.
Meyer, P., Waas, A.M., 2016. FEM predictions of damage in continous fiber ceramic matrix composites under transverse tension using the crack band method. Acta Mater. 102, 292–303.
Munro, R., 1997. Material properties .of a sintered α-SiC. J. Phys. Chem. Ref. Data 26, 1195–1203.
Nan, C.W., Clarke, D.R., 1996. The influence of particle size and particle fracture on the elastic/plastic deformation of metal matrix composites. Acta Mater. 44, 3801–3811.
Qu, S., Siegmund, T., Huang, Y., Wu, P.D., Zhang, F., Hwang, K.C., 2005. A study of particle size effect and interface fracture in aluminum alloy composite via an extended conventional theory of mechanism-based strain-gradient plasticity. Compos. Sci. Technol. 65, 1244–1253.
Roy, S., Gibmeier, J., Kostov, V., Weidenmann, K.A., Nagel, A., Wanner, A., 2011. Internal load transfer in a metal matrix composite with a three-dimensional interpenetrating structure. Acta Mater. 59, 1424–1435.
Shao, J.C., Xiao, B.L., Wang, Q.Z., Ma, Z.Y., Yang, K., 2011. An enhanced FEM model for particle size dependent flow strengthening and interface damage in particle reinforced metal matrix composites. Compos. Sci. Technol. 71, 39–45.
Sharma, N.K., Mishra, R.K., Sharma, S., 2016. 3D micromechanical analysis of thermo-mechanical behavior of Al2O3/Al metal matrix composites. Comp. Mater. Sci. 115, 192–201.
Shi, R., Nie, Z., Fan, Q., Li, G., 2016. Elastic plastic deformation of TC6 titanium alloy analyzed by in-situ synchrotron based X-ray diffraction and microstructure based finite element modeling. J. Alloy Compd. 688, 787–795.
Shibata, S., Taya, M., Mori, T., Mura, T., 1992. Dislocation punching from spherical inclusions in a metal matrix composite. Acta Metall. Mater. 40, 3141–3148.
Si, H., 2015. TetGen, a delaunay-based quality tetrahedral mesh generator. ACM Trans. Math. Softw. 41, 1–36.
Taya, M., Lulay, K.E., Lloyd, D.J., 1991. Strengthening of a particulate metal matrix composite by quenching. Acta Metall. Mater. 39, 73–87.
Wilkes, T.E., Harder, B.J., Almer, J.D., Faber, K.T., 2009. Load partitioning in honeycomb-like silicon carbide aluminum alloy composites. Acta Mater. 57, 6234–6242.
Young, M.L., Rao, R., Almer, J.D., Haeffner, D.R., Lewis, J.A., Dunand, D.C., 2009. Load partitioning in Al_2O_3–Al composites with three-dimensional periodic architecture. Acta Mater. 57, 2362–2375.
Zhang, J., Ouyang, Q., Guo, Q., Li, Z., Fan, G., Su, Y., Jiang, L., Lavernia, E.J., Schoenung, J.M., Zhang, D., 2016a. 3D Microstructure-based finite element modeling of deformation and fracture of SiCp/Al composites. Compos. Sci. Technol. 123, 1–9.
Zhang, J.F., Zhang, X.X., Wang, Q.Z., Xiao, B.L., Ma, Z.Y., 2017. Simulations of deformation and damage processes of SiCp/Al composites during tension. J. Mater. Sci. Technol.
Zhang, X.X., Ni, D.R., Xiao, B.L., Andrä, H., Gan, W.M., Hofmann, M., Ma, Z.Y., 2015. Determination of macroscopic and microscopic residual stresses in friction stir welded metal matrix composites via neutron diffraction. Acta Mater. 87, 161–173.
Zhang, X.X., Xiao, B.L., Andrä, H., Ma, Z.Y., 2016b. Multiscale modeling of macroscopic and microscopic residual stresses in metal matrix composites using 3D realistic digital microstructure models. Compos. Struct. 137, 18–32.
Zhang, X.X., Xiao, B.L., Andra, H., Ma, Z.Y., 2014a. Homogenization of the average thermo-elastoplastic properties of particle reinforced metal matrix composites: The minimum representative volume element size. Compos. Struct. 113, 459–468.
Zhang, X.X., Zhang, Q., Zangmeister, T., Xiao, B.L., Andrae, H., Ma, Z.Y., 2014b. A three-dimensional realistic microstructure model of particle-reinforced metal matrix composites. Model. Simul. Mater. Sci. Eng. 22.
Zhang, Y.B., Andriollo, T., Faester, S., Liu, W., Hattel, J., Barabash, R.I., 2016c. Three-dimensional local residual stress and orientation gradients near graphite nodules in ductile cast iron. Acta Mater. 121, 173–180.
Zhou, L., Huang, Z.Y., Wang, C.Z., Zhang, X.X., Xiao, B.L., Ma, Z.Y., 2016. Constitutive flow behaviour and finite element simulation of hot rolling of SiCp/2009A1 composite. Mech. Mater. 93, 32–42.